

Non-inductive plasma start-up on NSTX and projections to NSTX-U using transient CHI

This article has been downloaded from IOPscience. Please scroll down to see the full text article.

2013 Nucl. Fusion 53 073017

(<http://iopscience.iop.org/0029-5515/53/7/073017>)

View [the table of contents for this issue](#), or go to the [journal homepage](#) for more

Download details:

IP Address: 198.125.232.176

The article was downloaded on 10/06/2013 at 16:06

Please note that [terms and conditions apply](#).

Non-inductive plasma start-up on NSTX and projections to NSTX-U using transient CHI

R. Raman¹, D. Mueller², S.C. Jardin², T.R. Jarboe¹, B.A. Nelson¹, M.G. Bell², S.P. Gerhardt², E.B. Hooper³, S.M. Kaye², C.E. Kessel², J.E. Menard², M. Ono², V. Soukhanovskii³ and the NSTX Research Team²

¹ Department of Aeronautics and Astronautics, University of Washington, Seattle, WA, USA

² Princeton Plasma Physics Laboratory, Princeton, NJ, USA

³ Lawrence Livermore National Laboratory, Livermore, CA, USA

E-mail: raman@aa.washington.edu

Received 30 December 2012, accepted for publication 10 May 2013

Published 6 June 2013

Online at stacks.iop.org/NF/53/073017

Abstract

Transient coaxial helicity injection (CHI) in the National Spherical Torus Experiment (NSTX) has generated toroidal current on closed-flux surfaces without the use of the central solenoid. When induction from the central solenoid was added, CHI initiated discharges in NSTX achieved 1 MA of plasma current using 65% of the solenoid flux of standard induction-only discharges. In addition, the CHI-initiated discharges have lower density and a low normalized internal plasma inductance of 0.35, as desired for achieving advanced scenarios. Transient CHI will be used for non-inductive plasma start-up on the upgrade to NSTX (NSTX-U) that is now under construction. It will have numerous improvements that significantly enhance CHI start-up capability. The TSC code is now starting to be used for full discharge simulation, which includes solenoid-less start-up with CHI and subsequent non-inductive current ramp-up using neutral beams. These results suggest that the increased injector flux capability of NSTX-U should allow CHI start-up at more than the 400 kA level and that the new tangential neutral beam system on NSTX-U should be able to ramp the current to the 1 MA levels.

(Some figures may appear in colour only in the online journal)

1. Introduction

Tokamaks and spherical tokamaks (STs) have largely relied on a central solenoid to generate the initial plasma current and to sustain that current against resistive dissipation. However, a central solenoid cannot be used for plasma current sustainment indefinitely. The inclusion of a central solenoid in a tokamak for plasma start-up alone limits the minimum aspect ratio and adds cost and complexity. For fusion power plants based on the ST concept [1, 2], elimination of the central solenoid is necessary so alternative methods for plasma start-up would be needed.

The generation of toroidal plasma current by coaxial helicity injection (CHI) was originally developed for spheromak plasma formation [3] and has been used on several spheromak experiments including on the SSPX, CTX and RACE devices [4–6]. It has also been used in reconnection merging experiments [7, 8] and for spherical torus plasma formation [9, 10].

There are two approaches to CHI. In both approaches the toroidal current generated by CHI initially flows on open

field lines that connect two electrodes used for driving current with an external power supply, as described in section 2. For CHI to be able to produce toroidal plasma current on closed-flux surfaces magnetic reconnection must occur. In the first approach referred to as *steady-state* or *driven* CHI, closed-flux generation relies on the development of some form of non-axisymmetric plasma perturbation. This mode of CHI operation, in which the injector circuit is continuously driven for times longer than the timescale for resistive decay of the toroidal current ($t_{\text{pulse}} > \tau_{L/R}$) was initially studied in the early CHI experiments in National Spherical Torus Experiment (NSTX) [10]. Although substantial toroidal currents were generated using the steady-state approach, it was found that these discharges could not be successfully ramped up in current when induction was applied. This was due to an influx of low-Z impurities that increased the radiated power above the input power provided by induction.

However, complementary experiments on the HIT-II experiment at the University of Washington then demonstrated that a new mode of CHI operation in an ST, referred to as *transient* CHI could generate high-quality plasma equilibrium

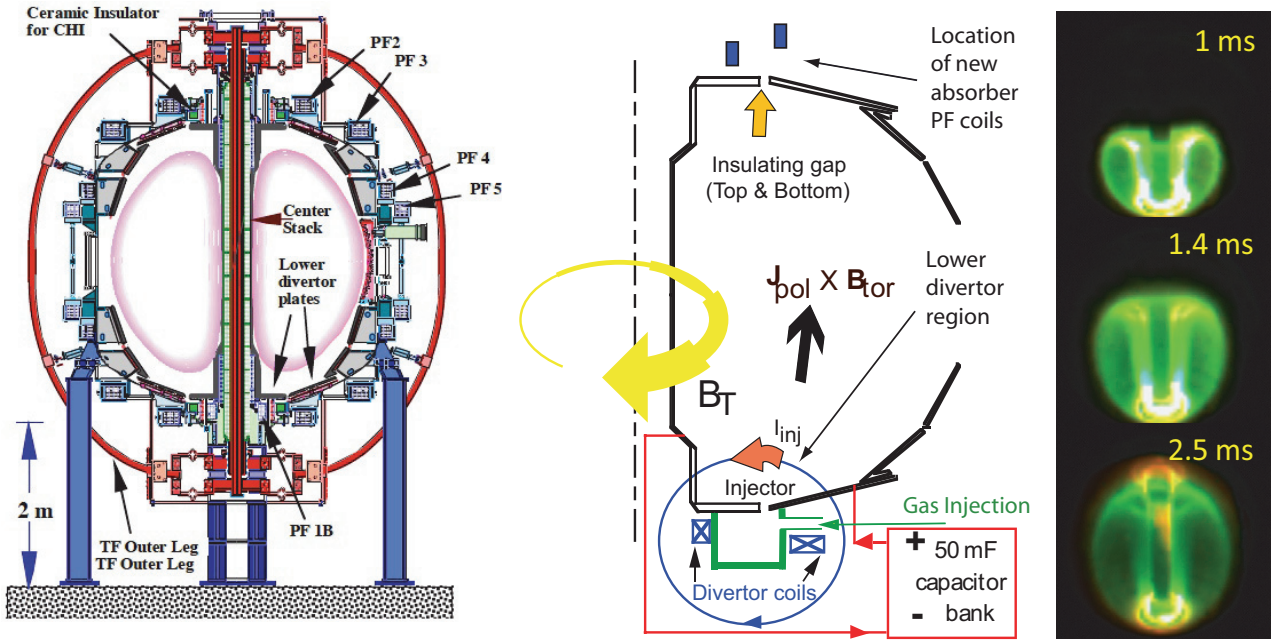


Figure 1. Shown are (left) drawing of the NSTX machine, (middle) cartoon of CHI start-up and (right) fast camera images of an evolving CHI discharge 1 ms, 1.4 ms and 2.5 ms after discharge of the CHI capacitor bank.

in a ST that could be successfully coupled to inductive drive as a result of reduced low- Z impurity influx [11]. While the *driven* CHI approach has the potential for steady-state current drive, for the purpose of initial plasma start-up, *transient* CHI [11], which involves only axisymmetric magnetic reconnection works very well and produces useful closed-flux equilibrium. In transient CHI, the initial poloidal field configuration is chosen such that the plasma carrying the injected current rapidly expands into the chamber. When the injected current is rapidly decreased, magnetic reconnection occurs near the injection electrodes; with the toroidal plasma current forming closed-flux surfaces. The method of transient CHI has now been successfully used on NSTX producing an unambiguous demonstration of closed-flux current generation without the use of the central solenoid [12].

Since that discovery, the transient-CHI method has been successfully applied to NSTX for solenoid-free plasma start-up followed by inductive ramp-up [13]. These coupled discharges have now achieved toroidal currents >1 MA using significantly less inductive flux than standard inductive discharges in NSTX.

Section 2 of this paper briefly summarizes the experimental results from NSTX. The numerous CHI system upgrades to the NSTX-U device are discussed in section 3 in the context of increasing the CHI current start-up potential. Section 4 discusses initial results from simulations with the TSC code that describes a scenario for full non-inductive start-up and ramp-up.

2. Experimental results

CHI is implemented in NSTX by driving current along field lines that connect the inner and outer lower divertor plates as shown in figure 1 and described in detail in [10–13]. During CHI operation, the divertor plates are used as electrodes. In NSTX the inner vessel and lower inner divertor plates are

the cathode while the outer divertor plates and vessel are the anode. Prior to initiating a CHI discharge the toroidal field coils and the lower divertor coils are energized. The lower divertor coils produce magnetic flux linking the lower inner and outer divertor plates, which are electrically isolated by toroidal insulators in the vacuum vessel. A programmed amount of gas is then injected into the vacuum chamber and voltage is applied between these plates, which ionizes the gas and produces current flowing along magnetic field lines connecting the plates. In NSTX, a 5–30 mF capacitor bank charged to 1.7 kV provides this current, called the injector current. As a result of the applied toroidal field, the field lines joining the electrodes wrap around the major axis many times so the injector current flowing in the plasma creates a much larger toroidal component, typically by a factor of 10–50 at the peak of the injector current in NSTX.

The maximum current multiplication (CM) that could be achieved in a ST device using CHI is related to the ratio of the toroidal flux in the CHI plasma to the injected poloidal flux, and is given by the relation $CM = \psi_T / \psi_{inj}$. This can be understood as the winding factor, which is similar to the parameter q , the number of times a field line goes around toroidally for a single transit along the poloidal direction. Thus, for a given injector flux, either increasing the toroidal field or the size of the device or both would increase the CM factor.

Significant improvement in the performance of CHI discharges in NSTX was achieved by reducing low- Z impurities, mainly oxygen and carbon in the initial electrode-driven discharge. Reference [13] describes this work in detail so the methods are briefly summarized here. The lower divertor plates, which are used as the CHI electrodes were initially cleaned using an extended electrode discharge. The CHI system itself was used for this purpose by running many discharges at high injector current but with significantly increased injector flux connecting the lower divertor plates. By maintaining the injector current below the level required

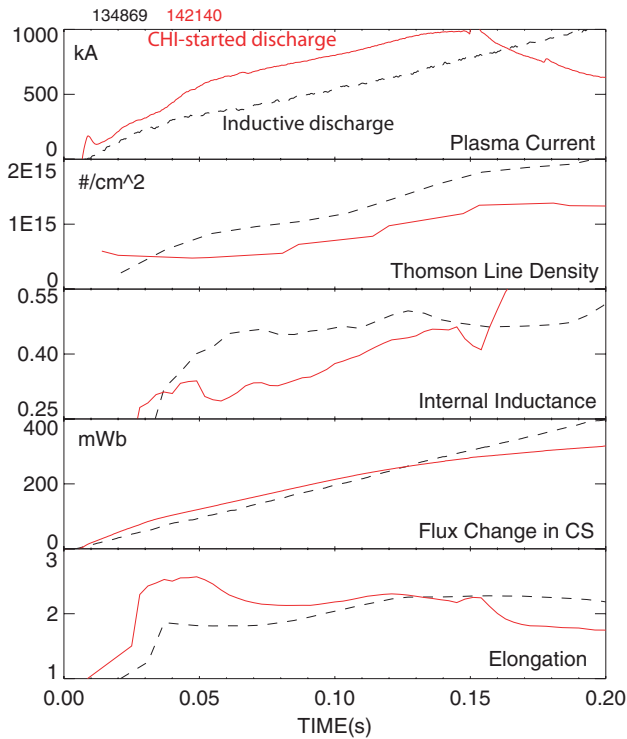


Figure 2. Comparison of time traces for discharges initiated with and without CHI start-up. The CHI-started discharge is essentially over by 150 ms, and begins an uncontrolled current decay starting at 150 ms. This is because the CHI-started discharge uses a unipolar central solenoid swing and so has available only half the solenoid flux of the reference NSTX discharge which uses bi-polar central solenoid swing. After about 140 ms, as the solenoid is reaching peak current for the CHI-started discharge, the available loop voltage provided by the solenoid drops to too low a level to sustain the discharge at the 1 MA levels. Thus at about 150 ms, the CHI-started discharge begins decaying (due to insufficient loop voltage), which causes the plasma to shrink. This is reflected by the decrease in elongation and increase in inductance seen after 150 ms.

(by MHD considerations) for ejecting the flux, the discharge was maintained near the lower divertor plates. This cleaning was followed by coating the lower divertor plates with lithium from a pair of evaporator ovens mounted at the top of the vacuum chamber, as described in [14]. Finally, during the CHI discharges, two poloidal field coils located in the upper divertor region were energized to provide a ‘buffer’ flux to reduce contact of the growing CHI discharge with the upper divertor electrodes [13]. Without this buffer flux, the growing CHI discharge could contact the upper divertor plates. This contact usually generated an arc between the upper divertor plates, which injected low-Z impurities into the CHI discharge, causing it to become more resistive which rapidly consumed the poloidal flux in the plasma.

Detailed results on the coupling of CHI-started discharges to induction are described in recent work [15, 16]. The results on the reduction in the central solenoid flux required to reach normal plasma current are briefly summarized here. In figure 2 we are comparing the plasma current trace for a CHI-started discharge ramped up by induction to a standard discharge initiated and ramped up by induction only. The inductive-only discharge is from the NSTX database, assembled over 10 years of operation that reached 1 MA in a shorter time than

other L-mode discharges. At 132 ms the CHI-started discharge consumes a total of 258 mWb of central solenoid flux to ramp up to 1 MA. At this time the reference inductive-only discharge gets to about 0.7 MA and it does not reach 1 MA until 190 ms, by which time 396 mWb of central solenoid flux had been consumed. Typical L-mode discharges in NSTX require at least 50% more inductive flux than discharges assisted by CHI.

Figure 2 shows that these plasmas have both a very high elongation of $\kappa \approx 2.6$ and very low internal inductance $l_i \approx 0.35$ from the start of the discharge. The CHI-initiated plasmas are relatively free of MHD activity despite having low density, which has previously been associated with increased instability during normal inductive start-up. Stability of CHI-started plasmas may also be due to high values of the safety factor q . While $q(0)$, q_{\min} have not been measured experimentally, equilibrium reconstructions of NSTX CHI discharges suggest values of about 8–12 for both parameters.

The lower internal inductance of CHI-generated discharges is associated with the formation of a hollow electron temperature profile, which is a characteristic of the CHI-start-up process which causes more of the current to flow in the outer region. This should also make it easier to control these plasmas because the current flowing in the plasma is effectively closer to the currents in the external equilibrium control coils. Many advanced operating modes for tokamaks strive to maintain a hollow current profile throughout the discharge both to reduce thermal transport and to maintain macroscopic plasma stability. That CHI is able both to provide an initial current profile similar to that which is achieved in conventional tokamaks through the use of high-power auxiliary heating, and to produce lower densities than achievable with conventional inductive start-up should benefit advanced scenario operations in NSTX-U.

3. Current start-up potential on NSTX-U

In a steady-state tokamak or an ST discharge that has no central solenoid, and is sustained non-inductively, it is necessary that the current start-up method must generate sufficient initial seed current so that it could be non-inductively ramped up to the levels required for sustained operation. Demonstrating this capability in support of a Fusion Nuclear Science Facility (FNSF) is a major objective of the NSTX-U program goals. On NSTX-U, the initial seed current will be ramped up using the three sources from a second more-tangential neutral beam system with tangency radius of 110, 120 and 130 cm. The increased tangency radius of injection increases the NBICD efficiency by depositing fast-ions on-average more parallel to the magnetic field. TRANSP calculations [17] show that the second more-tangential neutral beam system is far superior to driving current than the present beams that have smaller tangency radii and that the new beams would couple efficiently to targets with plasma currents as small as 300 kA. CHI, in NSTX-U, must therefore generate plasma currents of this magnitude.

In transient CHI, the maximum plasma current that the system can generate is directly proportional to the amount of poloidal injector flux the CHI system is capable of injecting into the vessel. This is because all of the poloidal flux the ST plasma contains at the end of the start-up phase must be

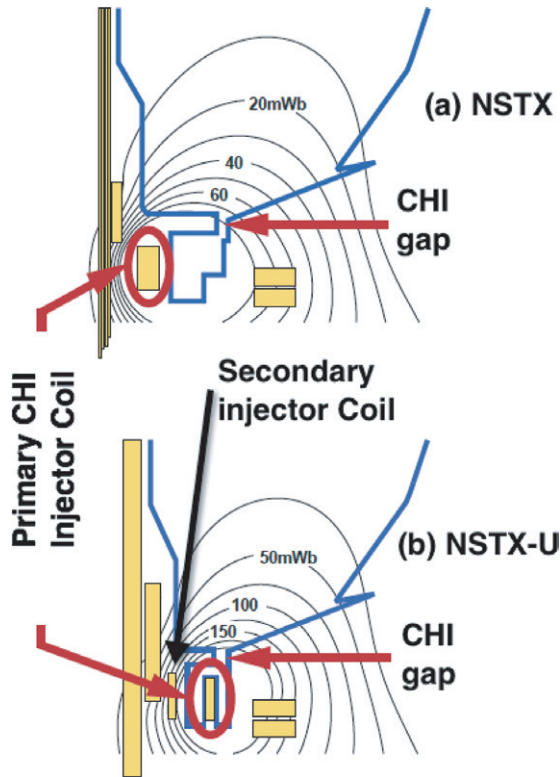


Figure 3. Injector flux contours for maximum allowed currents in the primary injector coil for (a) NSTX and (b) NSTX-U.

provided by the injector flux. In the absence of dynamo current drive there is no other mechanism to generate this closed field line poloidal flux during the very short 2–3 ms it takes CHI to establish the toroidal plasma current. Thus, in transient CHI, the injector flux places an upper limit on the magnitude of plasma current CHI can produce. Note from figure 1 that a mere 2.5 ms after the CHI capacitor bank has been discharged the CHI discharge has fully filled the vessel to form closed-flux plasma. In these discharges the plasma toroidal current (I_p) is related to the plasma poloidal flux through the relation $\psi_p = I_p R_p l_i \mu_0 / 2$. Here l_i is the normalized plasma internal inductance and R_p is the location of plasma major radius. For NSTX-like parameters with $l_i \sim 0.35$ and R_p of 0.93 m in NSTX-U, generating 400 kA of closed-flux plasma current requires injection of at least 82 mWb of poloidal injector flux. NSTX-U has two injector flux coils, as shown in figure 3. Use of both these coils allows for a maximum injector flux of 340 mWb in NSTX-U. This is considerably more than the injector flux capability in NSTX, which was 80 mWb. The reason for this substantial injector flux increase in NSTX-U is that the primary coil, the coil that is shown circled in figure 3, is much closer to the CHI gap in NSTX-U than in NSTX, this allows the injector flux from the injector coil to be used much more efficiently. Thus NSTX-U will have the capability to generate the 400 kA of closed-flux current that is needed for subsequent current ramp-up by the new tangential beam neutral system.

The maximum injector flux limits on NSTX-U suggest that transient CHI on NSTX-U may have the potential to generate close to the full 1 MA plasma current as this plasma would have a poloidal flux which is less than the injector flux limits on

NSTX-U. Increasing the CHI-produced plasma current, which requires injecting more poloidal injector flux requires higher levels of injector current. The minimum injector current, I_{inj} , required by CHI is related to the injector flux through the relation [18] $I_{inj} = 2\psi_{inj}^2 / (\mu_0^2 d^2 I_{TF})$. Here ‘ d ’ is the distance between the injector flux footprints on the divertor plates, I_{TF} is the current in the toroidal field coil and ψ_{inj} is the minimum injector flux that must be injected to generate a plasma with poloidal flux ψ_p , assuming there are no losses. Analysis of NSTX results shows that most of the injector flux (>70%) is retained as plasma poloidal flux, so the required injector flux values are about 30% more than the poloidal flux contained in the resulting plasma. Because of the increased toroidal field in NSTX (1 T versus 0.55 T in NSTX), for NSTX-U conditions injecting the amount of flux needed for a 400 kA discharge would require an injector current of about 13 kA, this is approximately the levels of injector current that could be driven in NSTX without impurity issues. The increased flux injection capability in NSTX-U at similar levels of the injector current used on NSTX is due to the higher toroidal field capability of NSTX-U, as reflected by the injector current relation. For comparison, the HIT-II experiment that had a much smaller electrode surface area, but due to better electrode surfaces, was able to drive 30 kA of injector current without impurity issues [19].

Impurity production from electrode surfaces is due to bombardment of material surfaces by plasma ions, which sputters atoms from the electrode surfaces into the plasma discharge. At a higher level of injector current the ion bombardment increases, as current is directly proportional to the amount of charge carriers. For NSTX graphite electrodes the primary impurities were carbon and oxygen that was adsorbed in the form of water. On HIT-II the anode was tungsten and the cathode was graphite that was largely free of water. At temperatures below 100 eV, the line radiation from metallic impurities is much less than that from low-Z impurities [20]. At temperatures of about 20 eV, line radiation from oxygen is much more than that from carbon [20]. It is because of reduced influx of oxygen on HIT-II, a much higher level of injector current could be driven on HIT-II. For graphite electrodes that contain adsorbed water, an effective way to minimize the influx of oxygen is to coat the entire surface of the electrode with lithium, as sputtering would then result in a predominantly lithium influx into the plasma, which has a much lower radiative cooling effect than oxygen [20]. The graphite electrodes on NSTX-U should have less adsorbed water than on NSTX, because NSTX-U will have capability to bake the divertor plates to a higher temperature than what was possible on NSTX. In addition, as described below, NSTX-U will have improved capability to more fully coat the divertor plates with lithium. These improvements on NSTX-U should allow NSTX-U to operate at injector currents higher than achieved on NSTX.

As briefly described in section 2, NSTX CHI research developed and utilized multiple methods for low-Z impurity control in CHI discharges. These methods will be further improved on NSTX-U, using new hardware capabilities; to further extend the magnitude of the CHI-produced plasma currents closer to the limits allowed by the injector flux coils. Initially NSTX-U will rely on full lithium coating of the lower

divertor surfaces. The results in figure 2 benefitted from only 50% coverage of the divertor surfaces with Li, so the increased Li coverage should have an immediate improvement on CHI discharges in NSTX-U. In addition, NSTX-U will have the capability to coat the upper divertor with Li. This has the benefit that during weak absorber arcs, which are usually present in high-current CHI discharges, Li will replace much of the oxygen impurity source. In addition to this, the ‘buffer flux’ NSTX coils used for reducing contact of the evolving CHI discharge with the upper divertor are twice as large on NSTX-U and have twice the current slew rate capability of the NSTX coils. These methods should allow the intrinsic CHI electron temperature to further increase beyond that achieved on NSTX. To synergistically add to these improvements, NSTX-U will be equipped with a 28 GHz 1 MW ECH system. GENRAY calculations indicate that the absorbed ECH power could be over 50% for CHI-like conditions, and preliminary calculations suggest that the CHI plasma electron temperature would increase by over 200 eV in 20 ms. At these temperatures, pre-programmed application of the 6 MW of high harmonic fast wave (HHFW) should boost the electron temperature substantially. Recent work on NSTX has shown that HHFW could increase the electron temperature of 300 kA plasmas from 200 eV to over 1 keV in less than 20 ms [21]. In addition to these improvements, it is also planned that after the start of initial plasma operations with graphite divertor tiles, molybdenum tiles will replace the lower graphite divertor tiles in NSTX-U. This should further reduce the influx of low-Z impurities. All of these improvements would act synergistically to enable NSTX-U to increase its capability for increasing the CHI-produced plasma current while reducing the impact of low-Z impurities.

4. TSC simulations

TSC is a time-dependent, free-boundary, predictive equilibrium evolution and transport code [22, 23]. It has previously been used for development of both discharge scenarios and plasma control systems. It solves fully dynamic MHD/Maxwell’s equations coupled to transport and circuit equations. The device hardware, coil and electrical power supply characteristics are provided as input. It models the evolution of free-boundary axisymmetric toroidal plasma on the resistive and energy confinement time scales. The plasma equilibrium and field evolution equations are solved on a two-dimensional Cartesian grid. Boundary conditions between plasma/vacuum/conductors are based on poloidal flux and tangential electric field being continuous across interfaces. The circuit equations are solved for all the poloidal field coil systems with the effects of induced currents in the passive conductors included. Currents flowing in the plasma on open field lines are included, and the toroidally symmetric part of this ‘halo current’ is computed. For modelling CHI in NSTX, the vacuum vessel is specified as a conducting structure with poloidal breaks at the top and bottom across which an electric potential difference is applied from which TSC calculates the injector current using a model for the resistivity of the ‘halo’ plasma. This circuit, however, contains a sheath resistance at each electrode, which is difficult to model. Since for the purposes of this study, it is the injector current and flux that are

important, we adopted the modelling strategy of adjusting the injector voltage in order to match the measured current rather than simply applying the measured injector voltage.

TSC simulations of NSTX transient-CHI discharges have successfully demonstrated current persistence [24], that is, the toroidal current persisting after the injector current has been reduced to zero. This generation of closed flux is the result of an effective (positive) toroidal loop voltage induced by the changing poloidal flux on the open field lines as the injector current is reduced to zero. Reference [24] provides additional details showing consistency with earlier theoretical predictions [18]. It also predicts that CHI scaling with toroidal field is favourable for larger machines. As described in section 3, the higher toroidal field allows more poloidal flux to be injected at lower levels of injector current, which decreases low-Z impurities.

This paper describes the first simulations of a fully non-inductive start-up scenario with CHI and subsequent non-inductive current ramp-up using neutral beams in support of planned experiments on NSTX-U. The CHI discharge is initiated in TSC as described in [24], and a closed-flux target of about 400 kA is established. This is the seed current that is subsequently ramped up using neutral beams. During the CHI-start-up phase, the first step involves current driven by the external injector circuit on purely open field lines. After this discharge fills the vessel, the applied CHI voltage is rapidly reduced. The resulting decrease in the injector current, which causes the injected poloidal flux to also decrease, induces a positive loop voltage that causes the generation of closed field lines carrying toroidal current. At the onset of flux closure a second step in the simulation is initiated. This continuously solves for the plasma boundary, including locating the divertor X-point, and begins solving the flux surface averaged transport equations. This phase begins 17 ms after the CHI discharge is first initiated. At 17 ms, horizontal position control is implemented to position and stabilize the CHI plasma on the outer passive plates. This is different from conventional inductive start-up in which the early plasma is usually positioned on the centre column, and the plasma is located much farther away from the equilibrium control coils than the CHI discharge is. Then, at 40 ms vertical position control is used to vertically centre the highly up/down asymmetric CHI plasma. As shown in figure 4, by 57 ms the CHI-initiated plasma is under full feedback equilibrium control. Experimental results from NSTX, shown in figure 2, relied on similar feedback control of the CHI discharge on similar time scales as used in these initial TSC simulations. The remaining two flux plots in figure 4 show that during the later parts of the non-inductive current ramp-up, as the plasma current increases, the discharge becomes elongated and fills the vessel.

For these simulations, the initial electron temperature for the CHI discharge is 100 eV. This is a reasonable starting value based on other simulations that show that 1 MW of 28 GHz ECH heating power (with 50% absorption efficiency) could rapidly increase the electron temperature of a CHI-like discharge to over 200 eV. The initial electron density is assumed to be $3 \times 10^{18} \text{ m}^{-3}$, similar to the densities obtained during CHI-start-up in NSTX, as shown in figure 2. In the simulation, the initial plasma internal inductance is below

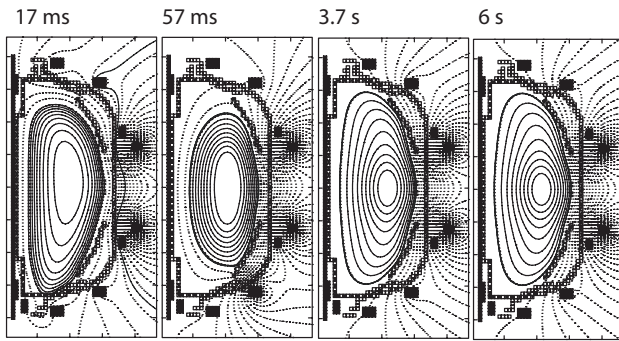


Figure 4. Poloidal flux contours from the TSC simulation showing the evolution of the flux surfaces at 17 ms, 57 ms, 3.7 s and 6 s and the corresponding plasma currents are 514 kA, 172 kA, 920 kA and 994 kA, respectively.

0.5, consistent with that calculated by EFIT for the CHI discharge in NSTX shown in figure 2. The CHI discharge, which is a low density, low inductance L-mode plasma is initially heated with 0.5 MW ECH and 2 MW of HHFW power. These are the magnitudes of the power absorbed by the plasma. The purpose of both these systems is to increase the electron temperature to the several hundred eV range for coupling to neutral beams as described in section 3. While HHFW could significantly contribute to current drive, in these initial simulations, we ignore any additional current drive from HHFW. During the first 200 ms, the density is kept low (below the cut-off density for ECH propagation and a Greenwald density fraction of less than 0.3), so that ECH can heat the discharge. Once the electron temperature exceeds 200 eV, ECH heating becomes less important as further temperature increases could be achieved using the HHFW system. By about 200 ms, the electron temperature exceeds 500 eV, after which the density is increased along with the neutral beam power. During the remaining current-ramp-up phase, as shown in figure 5(a), the electron density is maintained at about 0.6 times the Greenwald density fraction.

Figure 5(b) shows the evolution of the auxiliary heating from ECH + HHFW and NBI used in TSC. Figure 5(c) shows the plasma current components in these simulations. TSC uses fixed heating deposition profile shapes and efficiencies for the NBI CD, which is based on fits to TRANSP simulation results [17]. During the low density phase of the discharge the RF power is increased to 2.5 MW. This is assumed to be from a combination of 0.5 MW absorbed ECH power and 2 MW of absorbed HHFW power. After that 2 MW of HHFW power is retained in these simulations.

Figure 5(c) shows that during the initial 500 ms, neutral beam current drive is important in sustaining and slowing down the current decay. The coupled neutral beam power is assumed to be quite small during this phase (1.25 MW), primarily due to numerical restrictions within the TSC code that excludes formation of very hollow current profiles. In actual experiments, presumably the neutral beam power could be increased even further. At 0.34 s, an H-mode is initiated, after which the bootstrap + NBI currents exceed the equilibrium plasma current, and the plasma current is over-driven.

Starting from this time on, both the neutral beam power and the density are increased. This further increases the

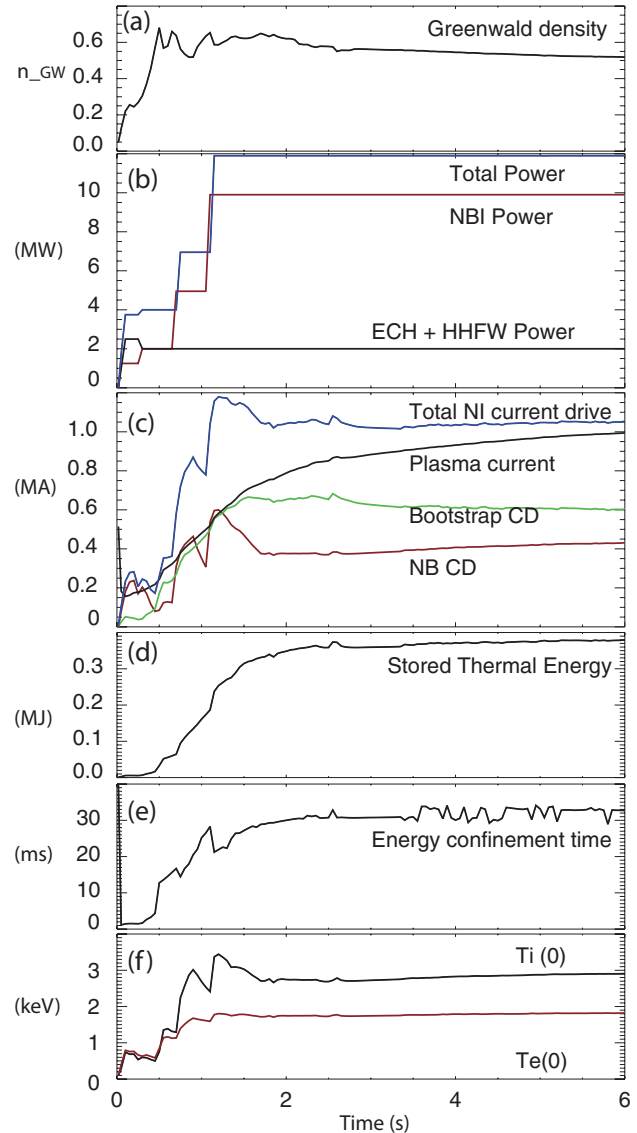


Figure 5. Shown are TSC results from a full discharge simulation that involves plasma start-up using CHI and current ramp-up using NBI and bootstrap current overdrive. Shown are (a) the Greenwald density fraction, (b) power traces for NBI, ECH + HHFW and the total non-inductive power, (c) current traces showing components of the total non-inductive current drive, plasma current, neutral beam driven current and the bootstrap driven current, (d) the plasma thermal energy, (e) the energy confinement time and (f) central electron and ion temperature.

bootstrap current and by 1 s, the combination of both these current drive terms exceeds 800 kA. By 2 s, the neutral beams and the bootstrap current contribute about 1 MA of current drive and the plasma current gradually ramps up to 1 MA at 6 s. During the NBI + bootstrap current overdrive phase, the increasing poloidal flux induces a negative loop voltage inside the plasma so the net current, which is the plasma current, increases on a slower timescale. Here we note that in these initial simulations, we have limited the plasma energy confinement time to be about 30 ms. During operation with lithium evaporative coatings, confinement times significantly in excess of 30 ms have been observed in NSTX [25]. At a higher level of the energy confinement time, the current will

ramp up faster than in this simulation, which should allow a period of non-inductive sustained operation in NSTX-U. These initial simulations have also ignored current drive from the application of HHFW. An alternative scenario would be to increase the amount of HHFW power during the initial 1–2 s and to benefit from additional current drive provided by HHFW. These future optimizations will study scenarios that strive to ramp the plasma current in less than the 6 s required in these simulations.

The Coppi–Tang L-mode transport model [23] is used in the initial L-mode phase. This transport model is improved with a reduced thermal diffusivity in the pedestal region to simulate an H-mode and give the profile shape observed in the high bootstrap-fraction phase of the H-mode in NSTX discharges. In both the L- and H-mode phases, the density profile shape is prescribed and has a peaking factor (defined as the ratio of the density at the magnetic axis to the volume averaged density) of approximately 1.1. The Z_{eff} value of 3.0 is also specified and is maintained constant in time and space.

Using these assumptions, figures 5(d) and (e) show the evolution of the stored plasma energy and the energy confinement time. The energy confinement time slowly increases to 30 ms at 2 s, after which it remains close to this value. The electron transport is adjusted to keep the energy confinement time at about 30 ms, consistent with energy confinement times in neutral beam-heated NSTX discharges. This value of τ_E is consistent with NSTX observations, although with Li conditioning, energy confinement times significantly exceeding 30 ms have been observed in NSTX. A higher confinement time would mean that beyond 2 s, a faster current ramp-rate would be maintained so that the discharge would reach 1 MA in less than the 6 s it takes in these initial simulations. The resulting central electron and ion temperatures are shown in figure 5(f), and have values of 1.7 keV for the electrons and 2.5 keV for the ions. T_i is significantly higher than T_e because, to be consistent with NSTX experimental observations, the ion thermal diffusivity is chosen to be 0.4 times the electron thermal diffusivity, because χ_i in NSTX is approximately neoclassical. The value of χ_i in these simulations varies from 1 to 10 m^{-2} , whereas the neoclassical value of χ_i in NSTX neutral beam-heated discharges is $1\text{--}5 \text{ m}^{-2}$ [26].

These initial studies with the TSC code give confidence that NSTX-Upgrade appears well equipped to study non-inductive current formation and ramp-up as needed for an ST-FNSF.

5. Summary and conclusions

The application of CHI on NSTX and on HIT-II combined with recent simulations with the TSC code has revealed many important aspects of CHI physics and its application to future machines, particularly the NSTX-U. The key results, not all of which are covered in this paper but are described in the supporting references, are briefly summarized below.

The 0.3 MA current generation in NSTX validates capability of CHI for high-current generation in a ST. Successful coupling of CHI-started discharges to inductive ramp-up and transition to an H-mode demonstrates compatibility with high-performance plasma operation. CHI

start-up has produced the type of plasmas required for non-inductive current ramp-up and sustainment. These are discharges with low internal inductance, low density and high elongation. The CHI scaling with increasing machine size is favourable for NSTX-U and to future devices.

The NSTX is now undergoing a major upgrade, to NSTX-U, to increase the capabilities of its toroidal and poloidal field coils and to add a second more tangentially injecting neutral beam line. Analysis of the NSTX results shows that the amount of closed-flux current generated by CHI is closely related to the initially applied injector flux. On NSTX-U the available injector flux is about 340 mWb, considerably exceeding 80 mWb in NSTX. The modelling projects that it should be possible to generate over 400 kA of closed-flux current with CHI in NSTX-U. At this current, the second more tangentially injecting neutral beam should be capable of providing sufficient current drive to ramp-up the plasma current. TSC simulations show that CHI could be an important tool for non-inductive start-up in next-step STs and quite possibly for tokamaks as well. NSTX-U is well positioned to develop full non-inductive start-up and current ramp-up in support of FNSF.

Acknowledgments

This work is supported by US DOE Contracts DE-AC02-09CH11466 and DE-FG02-99ER54519 AM08.

References

- [1] Najmabadi F. and the ARIES Team 2003 *Fusion Eng. Des.* **65** 143
- [2] Nishio S. *et al* 2004 *Proc. 20th IAEA Fusion Energy Conf. (Vilamoura, Portugal, 2004)* FT/P7-35 www.naweb.iaea.org/naweb/physics/fec/fec2004/datasets/index.html
- [3] Jarboe T.R. 1994 *Plasma Phys. Control. Fusion* **36** 945
- [4] Hooper E.B. *et al* 2012 *Plasma Phys. Control. Fusion* **54** 113001
- [5] Barnes C.W. *et al* 1990 *Phys. Fluids B* **2** 1871
- [6] Hammer J.H. *et al* 1991 *Phys. Fluids B* **3** 2236
- [7] Ono Y. *et al* 1996 *Phys. Rev. Lett.* **76** 3328
- [8] Brown M.R. *et al* 2008 *J. Fusion Energy* **27** 16
- [9] Nagata M., Kanki T., Fukumoto N. and Uyama T. 2003 *Phys. Plasmas* **10** 2932
- [10] Raman R. *et al* 2001 *Nucl. Fusion* **41** 1081
- [11] Raman R. *et al* 2003 *Phys. Rev. Lett.* **90** 075005
- [12] Raman R. *et al* 2006 *Phys. Rev. Lett.* **97** 175002
- [13] Raman R. *et al* 2010 *Phys. Rev. Lett.* **104** 095003
- [14] Kugel H.W. *et al* 2008 *Phys. Plasmas* **15** 056118
- [15] Raman R. *et al* 2011 *Phys. Plasmas* **18** 092504
- [16] Nelson B.A. *et al* 2011 *Nucl. Fusion* **51** 063008
- [17] Menard J.E. *et al* 2012 *Nucl. Fusion* **52** 083015
- [18] Jarboe T.R. 1989 *Fusion Technol.* **15** 7
- [19] Raman R. *et al* 2005 *Nucl. Fusion* **45** L15–19
- [20] Post D.E. *et al* 1977 Steady-state radiative cooling rates for low-density high-temperature plasmas *At. Data Nucl. Tables* **20** 397
- [21] Taylor G. *et al* 2012 *Phys. Plasmas* **10** 042501
- [22] Jardin S.C., Pomphrey N. and Delucia J. 1986 *J. Comput. Phys.* **66** 481–507
- [23] Jardin S.C., Bell M.G. and Pomphrey N. 1993 *Nucl. Fusion* **33** 371
- [24] Raman R. *et al* 2011 *Nucl. Fusion* **51** 113018
- [25] Maingi R. *et al* 2011 *Phys. Rev. Lett.* **107** 145004
- [26] Kaye S.M. *et al* 2009 *Nucl. Fusion* **49** 045010